HAL open science

Variability in Wood Quality and Moisture Content Measured by an Industrial X-Ray Scanner Across 700,000 Sawlogs of Picea abies, Abies alba, and Pinus sylvestris

Tojo Ravoajanahary, Romain Rémond, Renaud Daquitaine, Enrico Ursella, Jean-Michel Leban

To cite this version:

Tojo Ravoajanahary, Romain Rémond, Renaud Daquitaine, Enrico Ursella, Jean-Michel Leban. Variability in Wood Quality and Moisture Content Measured by an Industrial X-Ray Scanner Across 700,000 Sawlogs of Picea abies, Abies alba, and Pinus sylvestris. Forests, 2025, 16 (9), pp.1457. ⟨10.3390/f16091457⟩. ⟨hal-05252389⟩

HAL Id: hal-05252389

https://hal.inrae.fr/hal-05252389v1

Submitted on 12 Sep 2025

HAL is a multi-disciplinary open access archive for the deposit and dissemination of scientific research documents, whether they are published or not. The documents may come from teaching and research institutions in France or abroad, or from public or private research centers.

L'archive ouverte pluridisciplinaire **HAL**, est destinée au dépôt et à la diffusion de documents scientifiques de niveau recherche, publiés ou non, émanant des établissements d'enseignement et de recherche français ou étrangers, des laboratoires publics ou privés.

Distributed under a Creative Commons CC BY 4.0 - Attribution - International License

forests

MDPI

Article

Variability in Wood Quality and Moisture Content Measured by an Industrial X-Ray Scanner Across 700,000 Sawlogs of *Picea abies*, *Abies alba*, and *Pinus sylvestris*

Tojo Ravoajanahary [1,2,3,*], Romain Rémond [2], Renaud Daquitaine [1], Enrico Ursella [4] and Jean-Michel Leban [3,*]

[1] Groupe SIAT, 67280 Urmatt, France; renaud.daquitaine@groupesiat.fr
[2] Laboratoire d'Études et de Recherche sur le Matériau Bois, Institut National de Recherche pour L'agriculture, L'alimentation et L'environnement (INRAE), Université de Lorraine, 88000 Épinal, France; romain.remond@univ-lorraine.fr
[3] Institut National de Recherche pour L'agriculture, L'alimentation et L'environnement (INRAE), UR1138 Biogéochimie des Ecosystèmes Forestiers, 54280 Champenoux, France
[4] MiCROTEC, 39042 Bressanone, Italy; enrico.ursella@microtec.eu
* Correspondence: ravoajanaharytojo@gmail.com (T.R.); jean-michel.leban@inrae.fr (J.-M.L.)

Abstract

Evaluating sawlog quality is vital for both forest managers and wood processors. While external traits, such as tree form, branch architecture and visible growth features can be evaluated through visual inspection, many key wood quality indicators remain hidden, such as knot type and distribution, or the heartwood-to-sapwood ratio. This highlights the need for technologies capable of "seeing through" logs. Today, X-ray scanners in sawmills enable comprehensive, continuous, non-destructive assessment of internal stem structure at large scale. This study leveraged a newly compiled database of approximately 726,000 scanned logs to characterize variability in knot distribution and sapwood proportion across three major European softwood species and estimate the moisture content. The analysis highlights inter-and intra-species differences. Sapwood proportion decreased with sawlog diameter in spruce and silver fir but remained high in pine. Pine also presented significantly larger and more variable knots. Between March and August, we observed a seasonal trend in sapwood moisture content, affecting fresh density, while heartwood moisture content remained stable. These findings provide valuable information to support decision-making processes, linking tree characteristics to wood qualities and guiding forest management.

Keywords: wood quality; sapwood; knots; X-ray; computed tomography; *Picea abies* (L.) H. Karst.; *Abies alba* Mill.; *Pinus sylvestris* L.

Academic Editor: Alain Cloutier

Received: 31 July 2025
Revised: 1 September 2025
Accepted: 8 September 2025
Published: 12 September 2025

Citation: Ravoajanahary, T.; Rémond, R.; Daquitaine, R.; Ursella, E.; Leban, J.-M. Variability in Wood Quality and Moisture Content Measured by an Industrial X-Ray Scanner accross 700,000 Sawlogs of *Picea abies*, *Abies alba* and *Pinus sylvestris*. *Forests* **2025**, *16*, 1457. https://doi.org/10.3390/f16091457

Copyright: © 2025 by the authors. Licensee MDPI, Basel, Switzerland. This article is an open access article distributed under the terms and conditions of the Creative Commons Attribution (CC BY) license (https://creativecommons.org/licenses/by/4.0/).

1. Introduction

The efficient use of forest resources is fundamental for a sustainable bioeconomy, placing demands on the entire wood products value chain, from forest management to the final consumer [1]. Detailed understanding of sawlog quality is essential for both forest managers and wood processors. On one side, forest managers require information on how silvicultural practices influence tree growth and key wood properties to optimize stand value and guide genetic improvement programs [2]. On the other side, wood processors must accurately assess the characteristics of raw material in order to maximize

yield and product value by optimizing bucking and sawing strategies [3,4]. The objective is to achieve a more precise knowledge to better handle the natural variability of raw timber and the specific demand requirements for finished products, thereby reducing the volume of downgraded wood and increasing profitability [5]. This challenge is highlighted by the efforts on digitization of the wood industry sector, often termed Industry 4.0. For improving the online quality control, an increasing number of monitoring devices is implemented in the sawmills. This generates a large volume of data used for maximizing the value of the conversion process [6].

The primary obstacle to process optimization is the natural variability of wood. Key characteristics such as sapwood thickness [7], moisture content and density [8,9], and knot attributes are highly variable, influenced by species, genetics, and growth conditions like stand density [10,11]. Wood quality assessment has relied on external visual features and destructive analysis of small, often unrepresentative, samples. This manual approach is not only labor-intensive but has been shown to be inconsistent, with grader accuracy sometimes falling below 75% [12,13], resulting in an allocation of resources that is not optimal.

The integration of advanced scanning technologies, particularly industrial X-ray computed tomography (CT), has revolutionized the industry's capacity for non-destructive evaluation. The development of specialized industrial scanners allows for the creation of a "virtual log" before the first cut is made, a concept focused in research using X-rays for knot detection [14,15] and now realized in industrial practice [5,16]. These systems enable comprehensive, continuous data collection on internal sawlog attributes in a high-speed production environment, offering an unprecedented opportunity to analyze vast datasets [17].

Among the most critical internal features determining a sawlog's value are knots and the properties of sapwood and heartwood. Knots, as the main natural defect, directly influence both the mechanical strength and visual grade of lumber. Their presence creates stress concentrations that can compromise the integrity of structural components and engineered wood products such as glulam [18]. For this reason, knots are a primary reason for downgrading sawn timber in the context of structural applications [13]. However, knots are attracting growing scientific interest in the field of green chemistry due to their higher concentration of extractives [19–22], which can be used for the production of biobased chemicals. The development of algorithms for automated knot detection from CT data [23,24] and modeling their characteristics [10,25] are therefore active areas of research. The impact of a knot depends heavily on its status. Sound knots, originating from living branches, are structurally integrated with the surrounding wood, whereas dead knots, from deceased branches, represent discontinuities that are treated more severely in grading rules [26]. Previous research has highlighted the methodological importance of distinguishing between branch types to create robust predictive models. For instance, [27] demonstrated that separating living and dead branches was crucial for achieving model stability for Norway spruce across different regions in France. Following this principle, the present study analyzed sound and dead knots as distinct populations in order to depict the relationships between knots sizes and number and the sawlog geometrical characteristics.

Moreover, the sapwood-to-heartwood ratio is a decisive factor for many applications. The higher moisture content of sapwood impacts drying processes and energy consumption [28], while its lower natural durability and different coloration affect end-use suitability and aesthetic quality, especially for species like Scots pine where specific visual grading rules apply [7,8]. Furthermore, the basic wood density of these components is a quality indicator, as it is correlated with the stiffness and strength of the final product and is a key parameter in structural grading standards [13,29]. Given that wood density varies considerably from the stem base to the top and over time as a tree ages [29] and that it can be predicted from operational data [30], understanding its distribution within sapwood and heartwood is essential for accurately assessing wood quality and optimizing resource allocation.

Although numerous studies have been published on modeling the variations in wood properties, many are based on limited samples (sawlogs from 100 trees) and from laboratory-grade scanners. There is still a need to characterize the variability of key quality indicators using data from industrial scanners operating at a production scale. Such an analysis, grounded in a large dataset, can offer valuable insights into the variability of major commercial softwood species and serve as a foundation for developing accurate predictive models.

This study provides a new, comprehensive database containing data from approximately 726,000 sawlogs scanned online in the Groupe SIAT sawmill by an industrial MiCROTEC CT Log scanner. We quantified for each sawlog, the status (dead, sound) number, and size of knots and sapwood dimension for three major European softwood species: Norway spruce (*Picea abies* (L.) H. Karst.), silver fir (*Abies alba* Mill.), and Scots pine (*Pinus sylvestris* L.). The objective was to analyze this variability in order to create decision-making tools that can bridge the gap between forest management and industrial wood processing.

2. Materials and Methods

2.1. Dataset

This study analyzed production data collected over a six-month period, from March to August 2023, at the Groupe SIAT sawmill (Urmatt, France). The dataset is constituted of 726,895 sawlogs that were processed during this period. The data for each sawlog was acquired from an industrial CT scanner located at the sawmill's bucking unit. This scanner operated continuously and provided metric values of the internal wood quality averaged for each log. No specific preparation of the logs was performed for this study. After being scanned, the logs were not stored but were immediately conveyed to the sawing line as part of the continuous production process. Due to the posteriori nature of the data collection, specific details such as the pre-scanning storage duration or health status for each log could not be verified.

2.2. CT Log Scanner

CT scans were performed using the MiCROTEC CT Log scanner (Microtec, Bressanone, Italy), operating at 180 kV and 15 mA, with a transverse resolution of 1 mm, longitudinal resolution of 1 cm, and a scan speed of 126 m/min. CT Log images were processed by MiCROTEC's Interopt software (version 1.0) to extract stem shape and internal quality metrics at 10 cm intervals.

2.3. Wood Singularities Detection

The industrial CT Log scanner operates on the principle of differential X-ray attenuation. As wood is a heterogeneous material, X-rays are absorbed differently according to local variations in density and chemical composition. The system reconstructs a 3D density map of the sawlog, represented as a series of transverse tomographic images where grayscale variations and moisture content correspond to these density differences (Figure 1). The internal features are automatically detected and identified while the quality metrics are computed by the CT Log system. A brief overview of the principles behind the image analysis algorithms used in the Interopt software (version 1.0) is provided below; for more detailed information, readers can refer to the thesis [31].

(a) Heartwood–Sapwood delimitation

In fresh softwoods, sapwood has a higher moisture content than heartwood. This moisture difference results in a corresponding density variation that is visible on X-ray images, where the denser, high-moisture sapwood typically appears darker. To facilitate detection, the image is transformed into polar coordinates (distance from pith vs. angle),

as shown in Figure 1. Image median filters in radial and longitudinal direction are applied to smooth the data and reduce noise from fine details like grain texture. An algorithm then identifies a grayscale gradient along the radius (distance from pith), which marks the transition from heartwood to sapwood.

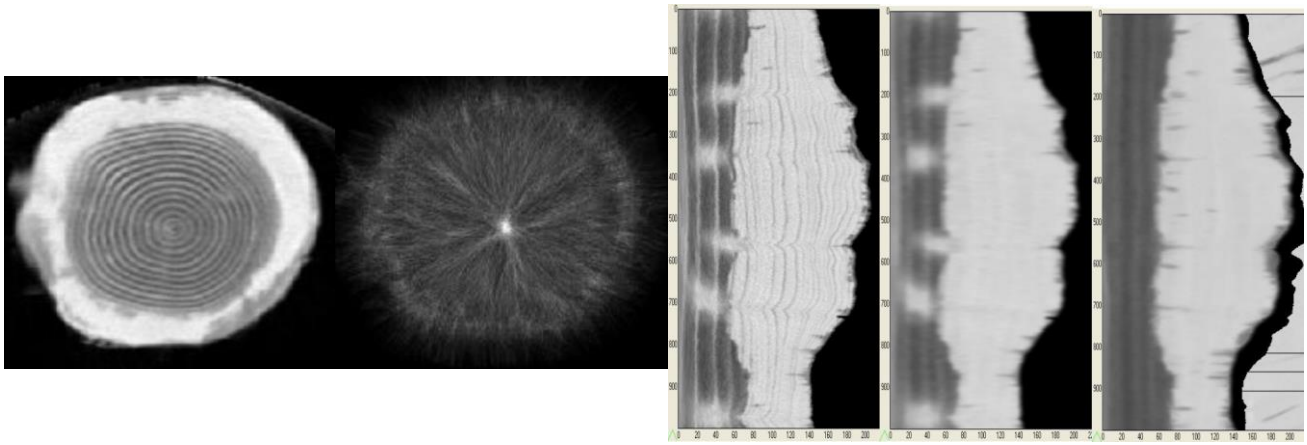

(**a**) (**b**)

Figure 1. (**a**) On left, CT slice with heartwood–sapwood and on right an example of pith detection using the Hough transform to find the convergence point of concentric annual rings. (**b**) Polar representation of a CT slice: in the abscissae, the distance from the pith, and in the ordinates, the angular position shows the transition from heartwood to sapwood (adapted from [31]).

(b) Knot detection and characterization

Knots, which are former branches embedded in the stem, typically have a higher density than the surrounding clear wood. Their shape is generally conical, extending from the pith toward the bark [32,33].

Initial knot identification relies on convolutional neural networks (CNN). These models are trained to recognize the characteristic density, texture, and shape patterns of knots in CT images and generate a 3D probability map of their locations within the sawlog.

Based on this probability map and the knowledge that knots originate at the pith, algorithms including Hough transform variants are used to identify the central axis of each knot. Once a knot's axis is located, a 3D zone around it is extracted for finer analysis:

- Dimensions: Other CNN-based algorithms analyze this zone to measure the knot diameter along its axis.
- Status (Sound/Dead): The distinction between a sound (living) and dead (black) knot is based on density and texture differences at the knot–wood interface. A sound knot is structurally integrated, while a dead knot is often encapsulated by a bark layer or poorly connected. Specialized CNN models, trained on data verified from sawn boards, classify sections of the knot as "sound" or "dead," allowing the delineation of the dead knot boundary. Finally, the number of knots per meter is calculated from the detected knots and the sawlog length.

Validation of the knots and sapwood detection are detailed in [31], in which they achieved 88% accuracy on knot status. On knot diameter, the standard deviation on difference between CT values and ground truth measurement was 3.2 mm and averaged −0.1 mm. Moreover, the validation of the metrics measured by the CT scanner was performed by the sawmill staff (unpublished results) when the CT scanner was installed in the sawmill.

2.4. Selected Descriptive Variables

The data from the scanner was exported into a readable format for spreadsheet software (e.g., Microsoft Excel). In the resulting dataset, each row corresponds to a single scanned sawlog, and the columns represent the measured variables, including sawlog identification, species, dimensions, and the synthetic indicators calculated for sapwood and knottiness (mean values for the entire sawlog).

The variables selected for this study were grouped into four main categories: (a) sawlog dimensions, (b) sapwood metrics, (c) knot metrics, and (d) density/moisture content.

(a) Sawlog dimensions

- Commercial diameter

For all subsequent analyses, the characteristic diameter used for each sawlog was its commercial diameter, i.e., the diameter at the mid-length of the sawlog, as illustrated in Figure 2. To analyze and compare the population structure, continuous stem diameter measurements were grouped into size classes. This approach facilitates the visualization of size distributions and allows for clearer assessment. A foundational class was created for all stems with a diameter less than 150 mm. Then, the class was established in 50 mm increments using left-inclusive intervals (e.g., [150, 200[, [200, 250[, etc.). The final category was an open-ended class that included all stems with a diameter of 550 mm or greater.

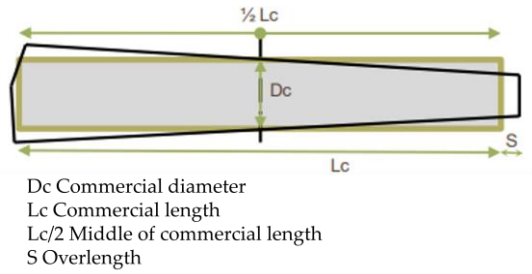

Figure 2. Method for calculating the commercial diameter of a sawlog according to the NF B53-020 standard [34].

- Length

The length is the distance from one end of the sawlog to the other (also in Figure 2).

(b) Sapwood dimensions

Figure 3 visually describes the corresponding measurement for each variable on the CT cross sectional images. For each scanned sawlog, the heartwood diameter was provided by the CT scanner. We modeled the heartwood as a circle using this value. From this and the section diameter, the sapwood width (SW) was calculated by subtracting the heartwood radius from the section radius.

$$\text{Sapwood width} = \text{section radius} - \text{heartwood radius} \quad (1)$$

Next, the cross-sectional areas of the sawlog, heartwood, and sapwood were calculated. The sapwood proportion is the ratio of the sapwood area to the total cross-sectional area.

$$\text{Sapwood proportion (\%)} = 100 * \text{sapwood area/section area} \quad (2)$$

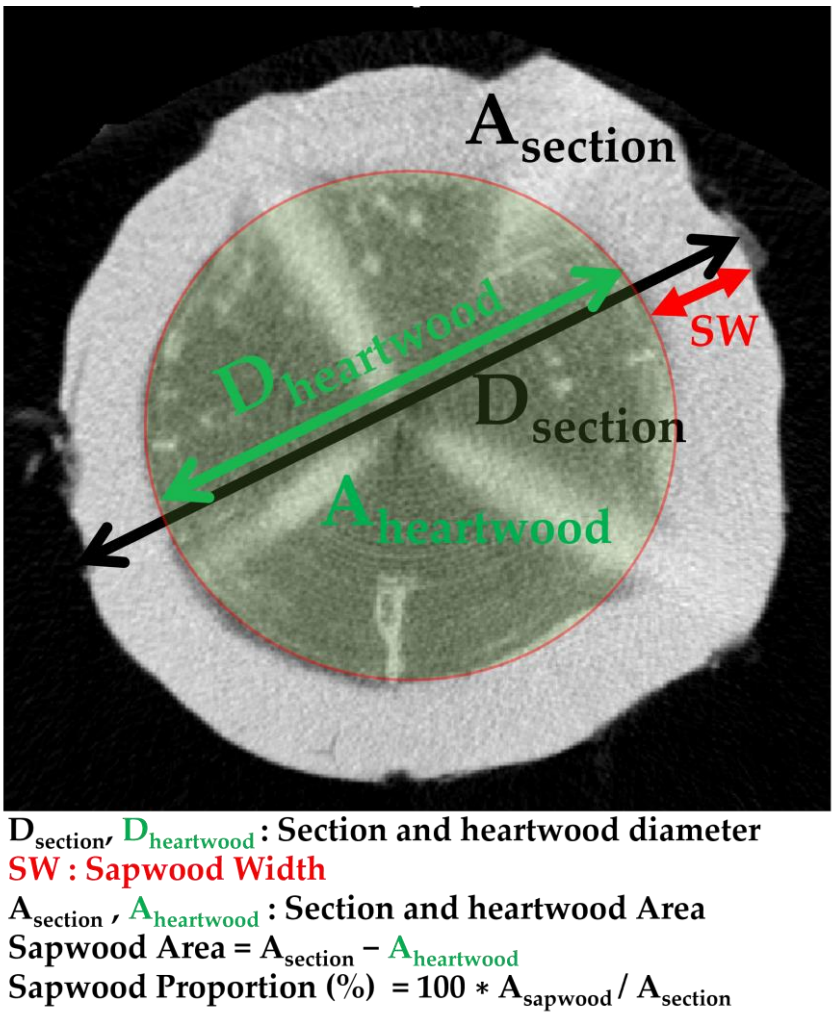

Figure 3. Illustration of the metrics measured on a scanned cross section. Light green circle represents the heartwood area. The border of the circle marked in red represents the transition to the sapwood.

(c) Knot dimensions and status

- Knot selection criteria (minimum diameter threshold)

The minimum knot size considered significant varies by sawmill, depending on the products and quality standards. For this study, a threshold of 7 mm in diameter was chosen. Only knots with a CT-detected diameter of 7 mm or larger were included in the metrics, such as the number of knots per meter and the average diameter used for optimization. This decision stems from the fact that knots smaller than this threshold are primarily small, inter-whorl knots, which have little impact on the quality and appearance of the sawmill's target products. Setting this threshold helps avoid overestimating the level of knottiness, which could otherwise lead optimization algorithms to unnecessarily downgrade logs or potential products.

- Average knot diameter

The diameter of a knot is defined as the average of its maximum diameter measured along the knot axis and its diameter measured perpendicular to that axis at its widest point. The average knot diameter for the sawlog is the mean of the diameters of all knots that meet the selection criteria.

- Knot status (sound vs. black)

The Figure 4 illustrates how knot diameters are measured based on their status when viewed from the tree's center (pith) to the bark. Sound knots, from a live branch, have a

uniform structure. The CT scanner measures their diameter at the widest point near the sawlog's surface (bark side). On the other hand, dead knot consists of two parts: the inner section that was once alive and the outer section that is dead. The CT scanner measures their diameter at the transition point where the live part of the knots ends and the decayed part begins.

- Number of knots per linear meter

This metric is not a simple average across the entire length of the sawlog; instead, it represents the maximum value obtained using a moving window approach. A virtual window, 1 m in length, is slid along the sawlog's axis. At each position, the number of knots that meet the defined selection criteria within that 1 m interval is counted. The final value reported in the CT measurement file is the highest knot count found throughout the sawlog. This calculation is performed separately for sound and dead knots.

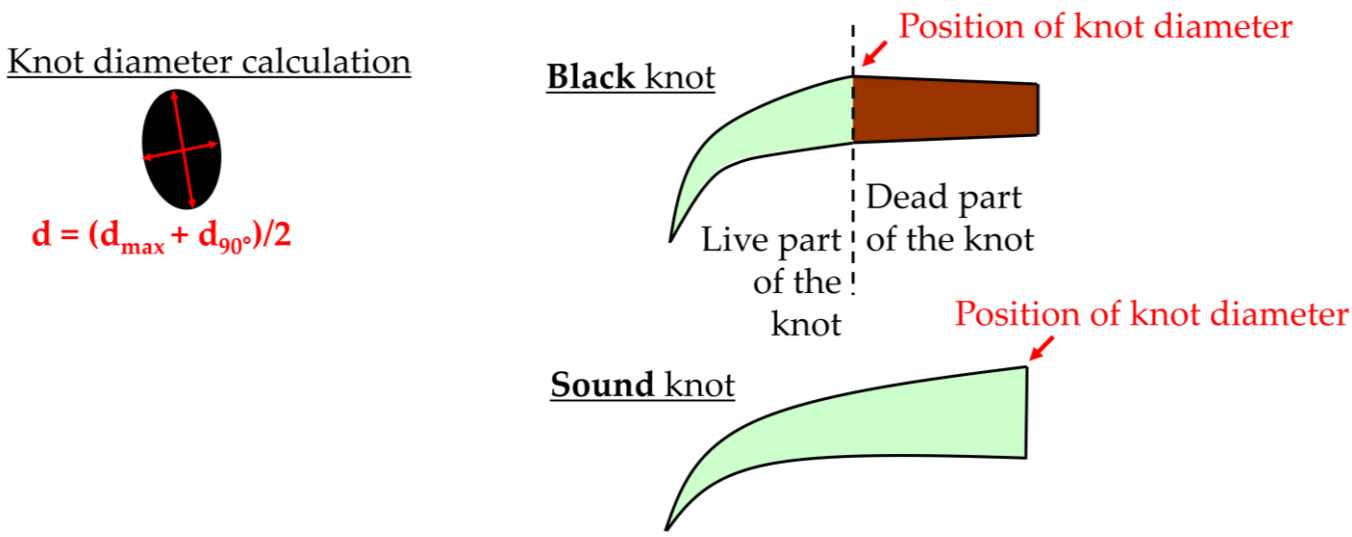

Figure 4. Diagram showing diameter calculus and its location measurement point for sound and black knots.

(d) Heartwood/sapwood density and moisture content

For each sawlog, mean density values for heartwood and sapwood were obtained directly from measurements performed by the CT scanner. These density values were then used to estimate the moisture content (MC) for both wood types. The MC calculation used a two-step, conditional formula to account for wood shrinkage below the fiber saturation point (FSP), which was assumed to be 30% for the species under study.

First, an initial MC was calculated by:

$$\mathrm{MC}\ (\%) = 100 * \left(\frac{\mathrm{density}_{[\mathrm{heartwood\ or\ sapwood}]}}{\mathrm{ID}} - 1\right) \tag{3}$$

where ID is the average basic density of wood, defined as the oven-dry mass divided by the saturated volume.

If the MC value was below the 30% FSP threshold, volume changes due to shrinkage had to be considered. A second formula was applied to correct these dimensional changes. Equation (3) was modified by incorporating the volumetric shrinkage coefficient (Rvt) to account for the linear relationship between the volumetric change of wood and variations in bound water content [35,36]:

$$\mathrm{MC}\ (\%) = 100 * \frac{(\mathrm{density}_{[\mathrm{heartwood\ or\ sapwood}]}/\mathrm{ID}) * (1 - \mathrm{Rvt}) - 1}{1 - \frac{\mathrm{density}_{[\mathrm{heartwood\ or\ sapwood}]}}{ID} * \frac{Rvt}{0.3}} \tag{4}$$

The species-specific basic density of wood (ID) and total volumetric shrinkage (Rvt) were obtained from the XyloDensMap data [37].

It is important to note that this MC calculation serves as an approximation for our study. The use of a single average ID and Rvt per species introduces some uncertainty, as both ID and Rvt vary between and within trees of the same species.

Consequently, the resulting MC values are intended to provide an estimate of the average relative variation and order of magnitude over the months of the study, rather than precise or absolute measurements for each sawlog.

2.5. Sample Description

Figure 5 shows the repartition of the study sample in function of the sawlog diameter classes for the three species. The dimensional characteristics of the 726,895 sawlogs analyzed in this study are summarized in Table 1. The sample included three species: pine (n = 9522), silver fir (n = 269,534), and spruce (n = 447,839). Overall, diameters were relatively consistent across species, whereas mean sawlog length was shorter for pine compared to spruce and silver fir.

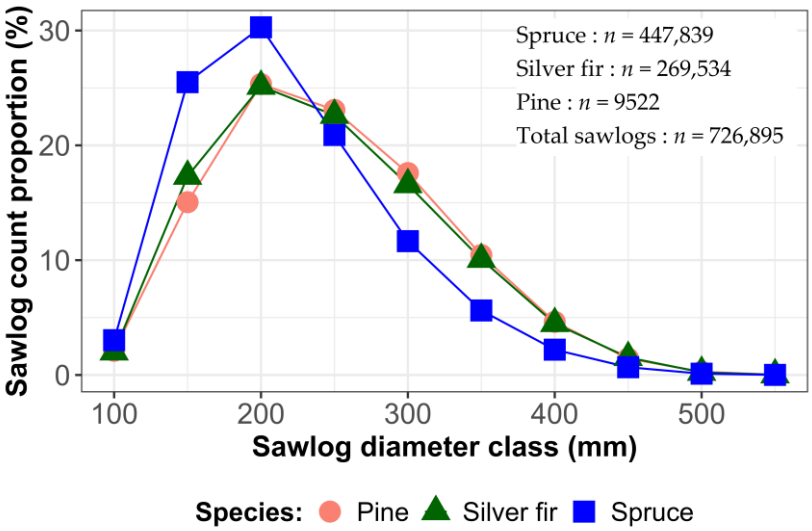

Figure 5. Distribution of sawlogs by diameter classes for the three studied species.

Table 1. Diameter and length of the study sawlogs (expressed as mean ± SD (min–max)).

Species	*n*	Diameter (mm)	Length (mm)
Pine	9522	269 ± 75 (100–580)	3368 ± 527 (2170–7020)
Silver fir	269,534	266 ± 76 (90–590)	4003 ± 823 (2020–8520)
Spruce	447,839	241 ± 69 (100–580)	4042 ± 765 (2120–8520)

2.6. Statistical Analysis

One limitation of the dataset of this study is the imbalance in sample sizes, with a relatively small number of pine logs. However, for sawlogs diameters higher than 400 mm, the number of samples in the smallest group (pine) is still n = 607, which is sufficient for basic statistical analysis. Nevertheless, a subsampling procedure was implemented. A balanced dataset was created by randomly sampling 9522 observations (total pine samples) from each of the three species. We used RStudio software ([38], version 2023.12.0 Build 369). The "seed" function in RStudio (set.seed(123)) was used to ensure that the random sampling is reproducible for each set of tests and make sure that the results are not biased by the over-representation of silver fir and Norway spruce.

(a) Sapwood proportion

An analysis of covariance (ANCOVA) framework compares the mean sapwood_proportion (the dependent variable) across the different species groups (the independent variable) while statistically controlling for the effect of diameter (the covariate). A crucial assumption for a standard ANCOVA model is the homogeneity of regression slopes, which postulates that the relationship between the covariate (diameter) and the dependent variable (sapwood proportion) is the same for all species. To test this, a model including an interaction term was fitted (sapwood_proportion ~ diameter * species). A significant interaction term ($p < 0.05$) indicates that this assumption is violated, meaning the slopes are not parallel. Therefore, the standard ANCOVA model could be inappropriate. The analysis must instead proceed with the interaction model. Interpretation then focuses on how the effect of the covariate (diameter) differs between the groups, rather than comparing overall adjusted means. Post hoc analysis using the emmeans package can be used to compare the slopes of the regression lines (emtrends function) for each species.

(b) Knot diameter variability

To assess the influence of tree species on knot dimension variability, a series of linear models were fitted to the data. The standard deviation of sound and black knot diameters was modeled separately as dependent variables; each tested against two predictors in separate models: sawlog diameter and mean knot diameter. To determine if the relationship between knot variability and the given predictor differed among pine, spruce, and silver fir, each model included an interaction term between the predictor and species. When a significant interaction effect was found ($p < 0.05$), post hoc pairwise comparisons were conducted to identify which species showed significantly different regression slopes. All analyses were performed on a balanced dataset to ensure comparability.

3. Results and Discussion

3.1. Sapwood Metrics

(a) Description of the metrics

Table 2 shows the descriptive statistics of the sapwood metrics and reveals distinct differences between species. Pine exhibited the highest mean sapwood width at 64 ± 24 mm, followed by silver fir at 58 ± 20 mm, and spruce, which had the narrowest sapwood at 41 ± 13 mm. This trend was reflected in the proportion of sapwood area, where pine also had the highest mean value (71 ± 15%), compared to silver fir (68 ± 15%) and spruce (57 ± 12%). Notably, pine also displayed the greatest variability in absolute sapwood width (SD = 24 mm), while spruce was the least variable in both its width (SD = 13 mm) and proportion (SD = 12%). These overall statistics confirm clear, species-specific patterns in sapwood characteristics.

Table 2. Sapwood metrics for the three species.

Species	*n*	Sapwood Width (mm)	Sapwood Proportion (%)
Pine	9522	64 ± 24 (18–178)	71 ± 15 (28–96)
Silver fir	269,534	58 ± 20 (13–212)	68 ± 15 (19–99)
Spruce	447,839	41 ± 13 (13–204)	57 ± 12 (17–98)

(b) Sapwood proportion

- For spruce and silver fir

For both spruce and silver fir, a clear decreasing trend in sapwood proportion was observed with increasing sawlog diameter (Figure 6). At any given diameter class, spruce consistently exhibited a lower sapwood proportion than fir. For example, in the 150 mm

diameter class, the sapwood proportion was approximately 65% for spruce and 75% for fir. This decreased to around 52% and 60%, respectively, in the 500 mm diameter class. This trend suggests that in these two species, the relative allocation of radial growth shifts with age. In the initial growth phase of trees, the cross-section of the trunks consists mainly of sapwood. As the trees age, heartwood gradually forms, particularly to provide mechanical support. The distinct difference between spruce and fir may reflect species-specific physiological strategies related to growth and water conduction.

- For pine

In contrast, the sapwood proportion for pine remained relatively high and more stable, starting around 80% and decreasing only slightly to approximately 70% in the 400 mm diameter class before appearing to increase again. This high sapwood proportion may reflect an adaptive strategy of this pioneer species, centered on efficient water conduction and delayed duraminization, likely enhancing its tolerance to various soil types. Pine maintains a high proportion of conductive xylem area, which can be accurately measured using techniques based on wood moisture content rather than staining methods [39]. This has direct implications for processing: large-diameter pine sawlogs will contain a proportionally larger volume of sapwood, which is less durable and non-colored, and has a higher moisture content. This directly affects the yield of colored heartwood and dictates different requirements for the drying process.

The knowledge of sapwood properties allows for more advanced sorting; larger sawlogs can be preferentially allocated to products where heartwood properties are desired by the customers. The authors of [7,40] also documented sapwood thickness variations in relation to tree characteristics, confirming that these patterns are inherent and could be predictable. The ability to model these species-specific trends provides a powerful tool for optimizing raw material allocation before the first cut is made.

(c) Sapwood width

For all three species, the mean sapwood width showed a clear increasing trend with sawlog diameter. However, the rate of increase differed. Pine consistently presented the greatest sapwood width, starting at approximately 40 mm in the 100 mm diameter class and increasing to more than 140 mm in the 550 mm class. Silver fir displayed an intermediate width, while spruce consistently had the narrowest sapwood, growing from roughly 30 mm to 80 mm across the same diameter range.

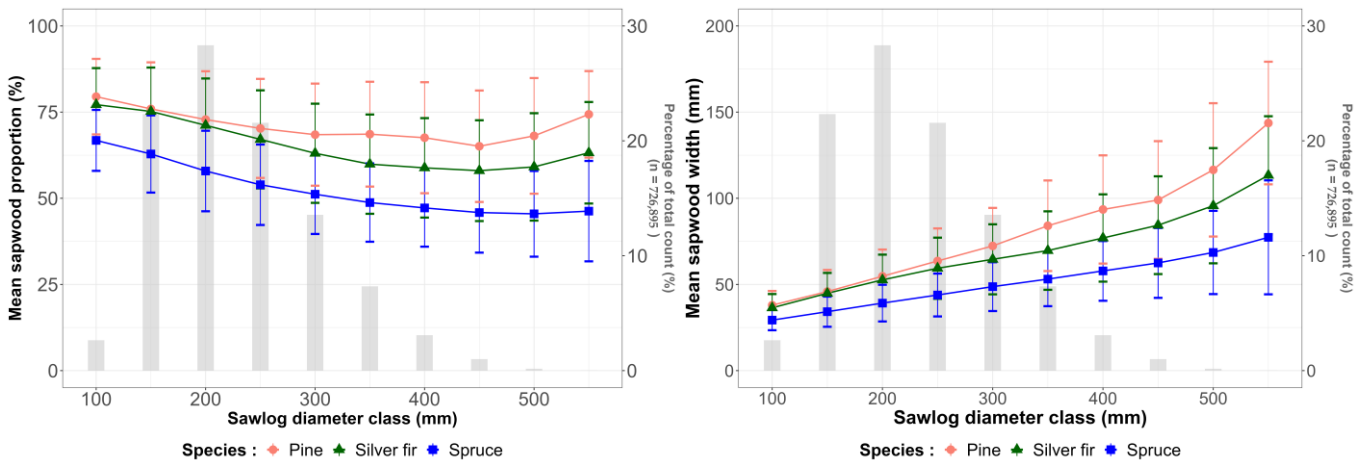

(**a**) (**b**)

Figure 6. Sapwood metrics in function of the sawlog diameter class for the three species. In (**a**) the sapwood proportion (%) and in (**b**) the sapwood width on the radius of the section. The grey bar, in secondary axis, is the percentage of total sample count.

It is important to note that for diameter classes exceeding 450 mm, the sample size for all species decreased substantially. Overall, 500 and 550 mm classes had 1164 and 77 samples respectively, across all species. The apparent upward trend in sapwood proportion for pine in the largest diameter classes, for instance, may not be representative of the general population and should be interpreted with caution due to the low number of observations.

(d) Statistical analysis

The test for the homogeneity of regression slopes, via the diameter and essence interaction term, was highly statistically significant ($F(2, 28{,}560) = 125.02$, $p < 0.001$). This finding indicates that the assumption of parallel slopes was violated. Therefore, the relationship between sawlog diameter and sapwood proportion was fundamentally different among the species. Because the interaction was significant, we analyzed the slopes from the interaction model as shown in Appendix A, Figure A1. The estimated slopes (the rate of change in sapwood proportion per mm of diameter) were pine: −0.038; silver fir: −0.073; spruce: −0.073.

A post hoc pairwise comparison of these slopes (Table A1) revealed that the slope for pine was significantly different from that of both silver fir ($p < 0.001$) and spruce ($p < 0.001$). However, the difference between slopes in silver fir and spruce was not statistically significant ($p = 0.9909$). This indicates that the sapwood proportion of pine decreased significantly more slowly with increasing sawlog diameter, whereas silver fir and spruce exhibited a statistically similar and steeper decline. This finding is critical for accurately modeling wood properties, as it shows that pine follows a distinct developmental pattern regarding sapwood proportion compared to spruce and fir.

3.2. Knots Metrics

(a) Description of the metrics

As detailed in Table 3, knot characteristics varied by species and type. Particularly, sound knots were larger in diameter than black knots for all three species, a trend that was most pronounced in pine. Pine sawlogs consistently presented the largest and most frequent sound knots. In contrast, spruce was characterized by having the smallest knots of both types and the lowest frequency of black knots. However, the knot diameters measured in our study are comparable in magnitude to those modeled for Scots pine and Norway spruce in other previous European studies [41,42].

Table 3. Variability of sound and black knots metrics (expressed as mean ± SD (min – max)).

Species	*n*	Sound Knots		Black Knots	
		Diameter (mm)	Number Per Linear Meter	Diameter (mm)	Number Per Linear Meter
Pine	9522	34 ± 12 (0–77)	5 ± 2 (0–14)	22 ± 9 (0–77)	3 ± 2 (0–16)
Silver fir	269,534	22 ± 7 (0–127)	4 ± 3 (0–26)	16 ± 5 (0–66)	4 ± 3 (0–24)
Spruce	447,839	20 ± 5 (0–154)	4 ± 3 (0–20)	13 ± 5 (0–61)	2 ± 2 (0–20)

(b) Dimensions of sound knots and variability

Figure 7 illustrates the variations in the average diameter of sound knots and their standard deviation as a function of sawlog diameter classes. For all three species, the average diameter of sound knots increased with sawlog diameter. Comparatively, as mentioned previously, pine tended to have the largest sound knots, followed by silver fir, with spruce having the smallest.

This marked increase directly reflects branch growth dynamics; branches that persist longer on larger trees, which are often older or have benefited from more growing space, reach larger dimensions. These findings are consistent with models for other conifer species that link larger branch and knot diameters to increasing tree size and stem diameter.

The standard deviation of sound knot diameter increased with the sawlog diameter class, indicating a greater dispersion of knot sizes in larger sawlogs. Pine was distinguished by higher variability compared to spruce and fir, which both exhibited similar levels of variation on this criterion.

This suggests greater heterogeneity in the development of living branches in pine. Such variability may stem from a broader range of branch vigor within the crown (e.g., a mix of dominant, vigorous branches and smaller, suppressed ones), a more plastic response to environmental conditions, or different genetic controls on growth. Indeed, several studies have highlighted significant genetic influences on growth traits in pine, which may contribute to this variability. This heterogeneity complicates the prediction of sawn timber quality from pine sawlogs and underscores the importance of detailed, individual sawlog assessment. It should be noted that the lower number of pine samples in this study could amplify the apparent heterogeneity.

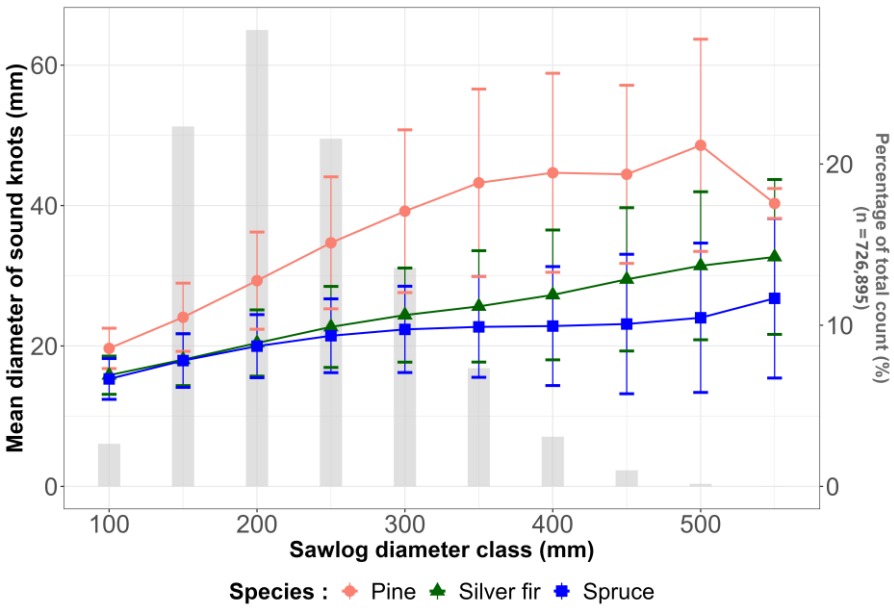

Figure 7. Mean sound knots diameter by sawlog diameter class for the three species. The grey bar, in secondary axis, is the percentage of total sample count.

(c) Dimensions of black knots and variability

Figure 8 shows the relationship between the mean diameter of black knots and the sawlog diameter class for the three species. A positive correlation was observed for all species, where the average diameter of black knots increased with sawlog diameter. This trend may reflect, in part, biological processes such as crown dynamics, where dominant trees develop larger branches that persist longer before dying due to crown recession and natural pruning. It may also result from the fact that large-diameter sawlogs are often taken from the lower part of the stem (i.e., butt logs), where older and larger branches had formed early in the tree's development, before being naturally pruned. The resulting black knot diameter therefore corresponds to the maximum size the branch achieved while it was alive. In inter-species comparison, pine consistently presented the largest black knots, followed by silver fir, with spruce having the smallest.

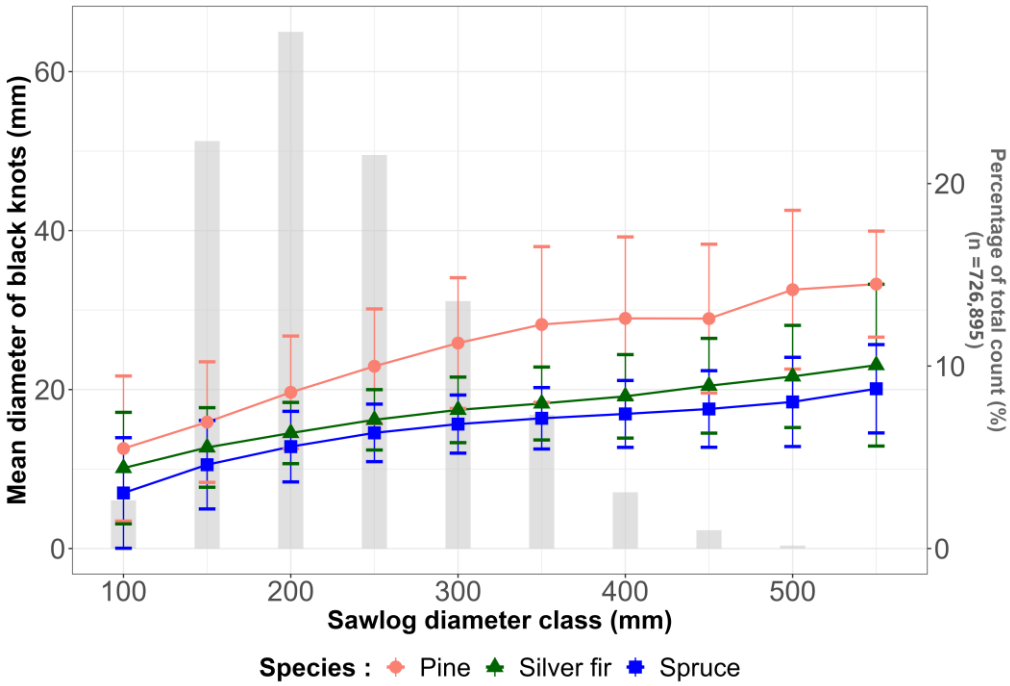

Figure 8. Mean black knots diameter by sawlog diameter class for the three species. The grey bar, in secondary axis, is the percentage of total sample count.

The variability in black knot diameter, indicated by the standard deviation, also increased with sawlog diameter class. This suggests a greater range of dead branch sizes being occluded within larger sawlogs. Pine was distinguished by higher variability compared to silver fir and spruce, which showed more constrained and similar levels of variation. This pronounced heterogeneity in pine likely reflects a greater plasticity in its response to stand density and competition for this pioneer species, leading to more diverse branch growth and mortality scenarios. This high variability in a key wood defect complicates quality assessment based on external sawlog features alone and stresses the challenge in predicting the final grade of sawn timber from pine.

(d) Number of sound and black knots per linear meter

Figure 9 shows that the number of sound knots per linear meter decreased as sawlog diameter increased for all three species. The reason is that large-diameter sawlogs in the wood supply are typically butt sawlogs, from which lower branches have naturally shed over time, resulting in fewer sound knots from the original living crown. In contrast, small-diameter sawlogs are often top sawlogs that originate entirely within the live crown, where nearly all knots are sound. This distinction between the living crown and the dead branches is critical for accurately modeling knots characteristics. Among the species, silver fir exhibited the highest density of sound knots, particularly in the intermediate diameter classes.

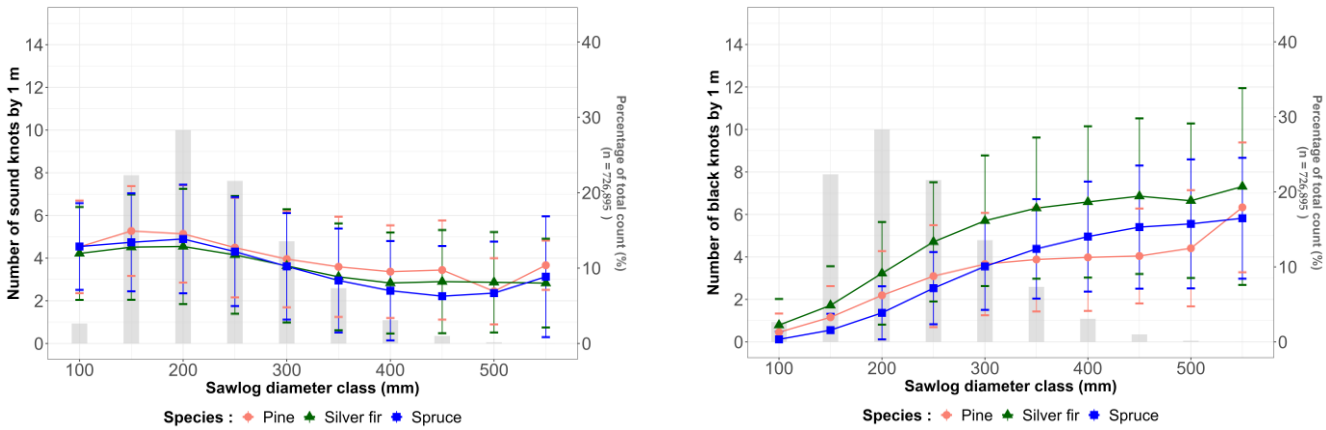

(**a**) (**b**)

Figure 9. Number of knots per linear meter, (**a**) for sound knots and (**b**) for black knots. The grey bar, in secondary axis, is the percentage of total sample count.

(e) Statistical analysis

The ANCOVA test was found significant for the linear models of both black and sound knots, showing that there was no homogeneity of the regression slopes. Therefore, there was an interaction of the species on knot variability.

The analysis investigated how knot diameter variability is influenced by tree species, sawlog diameter, and mean knot size. All four linear models were highly significant ($p < 0.001$), explaining 66–79% of the variance (adjusted R^2) in knot standard deviation (Figure 10). The summary of the models is available in Appendix B, Table B1. The key findings relate to the moderating effect of species on these relationships.

- Influence of sawlog diameter on knot variability

A significant interaction was found between sawlog diameter and species for both black and sound knot variability, indicating that the relationship between sawlog size and knot variability differs among species. For black knots, the variability in spruce increased significantly less with sawlog diameter compared to pine ($p = 0.005$). The trend for silver fir was not significantly different from pine. For sound knots, the increase in variability with sawlog diameter was significantly steeper for pine than for either silver fir ($p < 0.001$) or spruce ($p = 0.004$). The slopes for silver fir and spruce did not differ significantly from each other.

- Influence of mean knot diameter on knot variability

The relationship between the mean diameter of knots and their standard deviation (a measure of heteroscedasticity) was also significantly moderated by tree species. The variability of black knots in spruce showed a significantly different relationship with mean knot size compared to that of pine ($p = 0.003$). Specifically, the slope of this relationship was less pronounced for spruce. A similar interaction was observed for sound knots, where the relationship between mean size and variability for spruce was significantly different from that of pine ($p = 0.010$). In this case, the variability in sound knots increased more sharply with their mean size in spruce than in pine.

Pine consistently showed the strongest positive relationship between sawlog diameter and sound knot variability. Furthermore, the relationship between mean knot size and its own variability was distinct for spruce compared to pine and silver fir, particularly for sound knots.

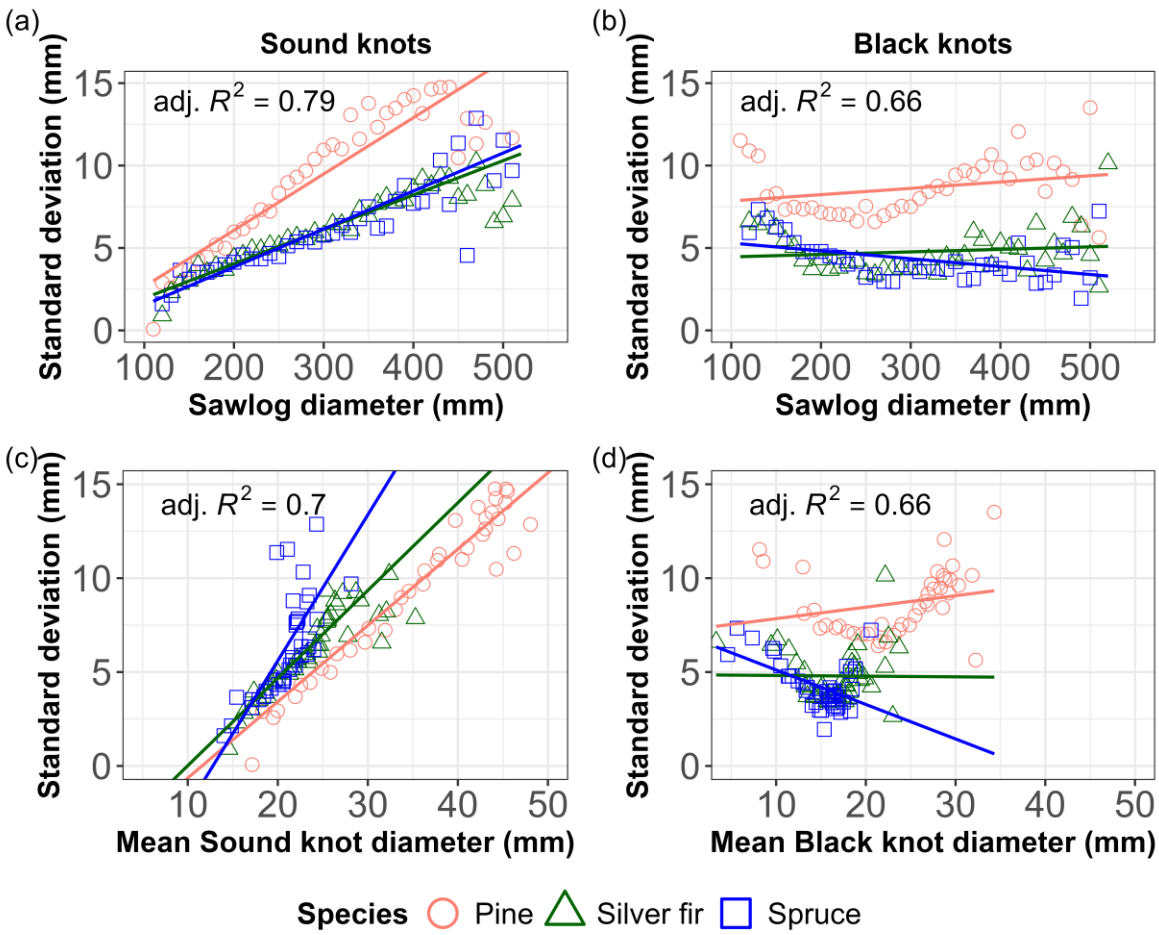

Figure 10. Standard deviation (SD) of knot diameters vs. (**a**) sawlog diameter for sound knots, (**b**) sawlog diameter for black knots, (**c**) mean sound knot diameter, and (**d**) mean black knot diameter. Some overlaps occur due to high data density.

3.3. Sapwood and Heartwood Density and Moisture Content

The seasonal data, presented in Figure 11, reveals distinct and physiologically trends in wood moisture content (MC) and density for all three species, particularly within the sapwood.

In Table 4, the analysis shows a pronounced difference in moisture content (MC) between the two wood types across all three species. Sapwood consistently exhibited substantially higher MC, with mean values ranging from 93% for pine to 105% for silver fir. In contrast, heartwood was drier, with mean MC values between 23% (spruce) and 43% (silver fir). This clear distinction aligns with the primary physiological roles of sapwood in water conduction and heartwood in structural support.

The species ranking in our data (silver fir > spruce > pine) are similar in the XyloDensMap reference data [37]. Silver fir is the species with the highest moisture content in both datasets. Furthermore, the maximum MC values recorded in our study (136–172%) show correspondence with the maximums reported in XyloDensMap (150–180%), suggesting a similar upper limit for moisture saturation across the species.

Table 4. Moisture content (MC) of heartwood and sapwood for the species studies with MC values from XDM data.

Species	*n*	Heartwood		Sapwood		XyloDensMap MC	
		Mean ± sd (%)	Max (%)	Mean ± sd (%)	Max (%)	Mean (%)	Max (%)
Pine	9522	29 ± 23	131	93 ± 28	136	70	150
Silver fir	269,534	43 ± 22	174	105 ± 35	158	98	170
Spruce	447,839	23 ± 19	168	100 ± 42	172	60	180

(a) Seasonal dynamics of moisture content in sapwood

The most noticeable trend observed across spruce, silver fir, and pine was a consistent and marked decrease in sapwood moisture content from early spring (March) to late summer (August). For all species, sapwood MC began at its peak, typically between 110–120% and progressively declined to 70–85% by August. This pattern directly corresponds to the seasonal cycle of tree physiology. The high initial MC in spring reflects the mobilization of water for budbreak and the onset of transpiration. As the summer progresses, higher temperatures and increased evapotranspiration rates lead to a gradual desiccation of the sawlogs post-harvest, a well-documented phenomenon as initial moisture content is typically high, especially in sapwood, and decreases over time due to drying [43,44]. This seasonal variation in wood MC has practical implications for the timber industry, as it affects both the sawlog weight during transport and the amount of water evaporated during the drying of sawn products. Managing a log yard effectively requires adapting to these seasonal supply variations [45].

(b) Contrasting seasonal behavior of sapwood and heartwood MC dynamics

In contrast to the dynamic nature of sapwood, the heartwood in all three species demonstrated remarkable stability in both moisture content and density throughout the observation period. Heartwood MC remained low and relatively constant, typically ranging between 25% and 45%, with minimal variation. This stability is expected, as heartwood is composed of non-living cells and does not participate in active water transport [46]. Studies on various softwood species show that sapwood typically has higher initial moisture content and drying rates than heartwood [47]. This fundamental physiological difference highlights the contrast between the water-conducting sapwood and the inert, structurally focused heartwood. It is worth noting that the low MC observed in the heartwood, sometimes falling below the fiber saturation point (FSP), may partially reflect drying that occurred between tree felling and the CT scanning.

(c) Inter-species variations

While the overall trends are similar, subtle differences between species are apparent.

Silver fir and spruce showed very similar patterns: a steep, consistent decline in sapwood MC and highly stable heartwood properties. This suggests a comparable physiological response to seasonal changes and post-harvest drying.

Pine displayed a slightly more different pattern, particularly in its heartwood. A minor but noticeable increase in heartwood MC was observed from April to July. While the variability was large, this could be an artifact of the smaller sample size for this species in certain months as indicated by the sawlog count bars. Furthermore, the initial sapwood MC in pine appeared slightly lower, likely due to its reduced porosity compared to the other two species.

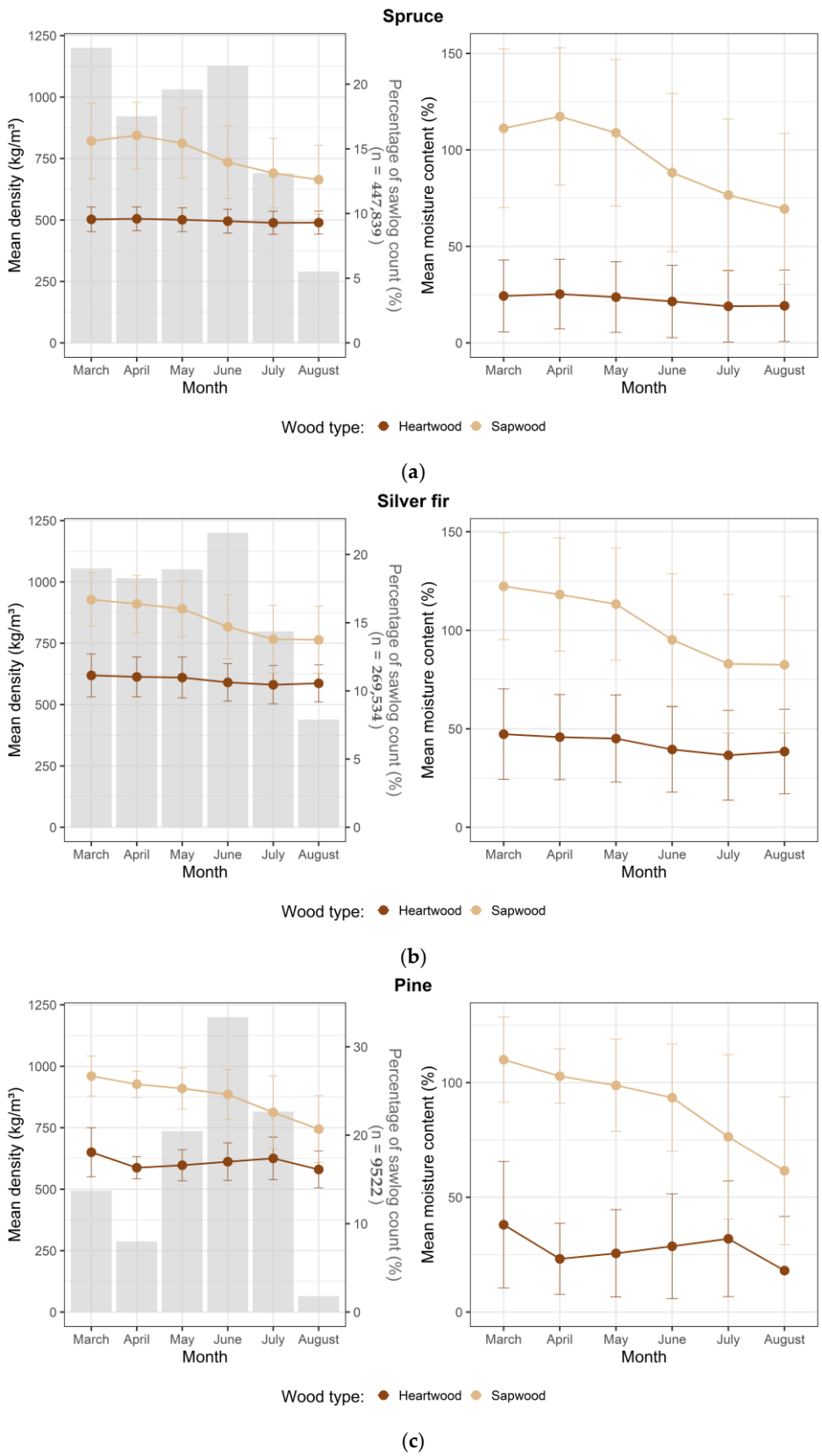

Figure 11. Mean densities (**left**) and MC (**right**) of heartwood and sapwood for each species: (**a**) spruce, (**b**) silver fir, and (**c**) pine. The grey bar, in secondary axis, is the percentage of total sample count.

3.4. Current Limitations

While this study is based on an exceptionally large dataset, it has certain limitations. The sample sizes were imbalanced across the three species. These factors may affect the

robustness of the observed trends at the upper end of the sawlog diameter range. Future work should aim to increase the number of sawlogs for the higher sawlog diameter classes. Moreover, further work ongoing will focus, from a statistical point of view, on the variations of quality metrics (means and standard deviations) in relation to the number of measured sawlogs.

It is also important to acknowledge the absence of information on the health status of the study sample as a potential limitation of this method. In fact, confounding effect of fungal decay, such as butt rot caused by *Heterobasidion annosum* [48], on density readings, and consequently on MC estimation, warrants further investigation. Similarly, colonization by bark beetles like *Ips typographus* also warrants consideration as the fungi they introduce are known to alter wood's physical properties [49]. Over time, these fungal infestations can cause weight loss and increase wood permeability, which would also introduce variability into density-based moisture content estimations.

Additionally, another limitation of this study is the method used to estimate MC. The calculation relied on a single, species-specific average basic density (ID) sourced from the XyloDensMap database [37]. This approach, while based on a large and reliable dataset, does not account for the natural, inter-tree variability in basic density that exists within any given species. This simplification may contribute to the notably low mean MC values observed, particularly in the heartwood of spruce, which were lower than typically expected. Due to the industrial and retrospective nature of the data collection, direct verification of these values on the study sample was not possible.

Nevertheless, the methodology is grounded in established physical principles and standard formulas [35]. While the absolute MC values should be interpreted with caution, the primary value of these results lies in their relative comparisons and observed trends. The contrast between sapwood and heartwood dynamics, the clear seasonal decline in sapwood MC, and the comparative differences between the three species are robust and physiologically consistent findings. Therefore, the results serve as a valid, large-scale indicator of seasonal and structural moisture dynamics, even if the absolute precision for any single log is limited. Future work will aim to incorporate more direct MC measurement techniques to refine and validate these estimations.

4. Conclusions

This study successfully leveraged a massive industrial CT scanner dataset to provide a comprehensive, quantitative characterization of key wood quality indicators for three major European softwood species. By analyzing for the first time nearly 726,000 sawlogs, we have detailed the intrinsic variability of sapwood, sound knots, and dead knots, providing a critical foundation for bridging the gap between raw material assessment and value-optimized industrial processing.

Our key findings and perspectives are:

- Distinct species patterns:

  The three species—Norway spruce, silver fir, and Scots pine—showed fundamentally different patterns in wood structure. For instance, the proportion of sapwood decreased with increasing sawlog diameter in spruce and fir, while it remained consistently high in pine. Additionally, pine was characterized by significantly larger and more variable knots than spruce or fir, a trait linked to its specific genetics and growth strategies.

- Contrasting patterns of size and number variations for both sound and dead knots:

  The dynamics of sound and black knots were distinct and often inversely related to sawlog diameter. The frequency of sound knots tended to decline in larger-diameter butt sawlogs, which contain a growing number of dead knots resulting from natural

pruning and crown rise. This confirms that the two knot types result from different biological processes—active branch growth versus branch mortality—and should be modeled as separate populations to more accurately predict sawlog quality.

- Seasonal variation in sapwood moisture content (MC):

  A clear seasonal trend was observed in the fresh density of sapwood, primarily driven by fluctuations in moisture content. In contrast, heartwood MC remained nearly constant throughout the year. This temporal pattern, consistent with known physiological processes, was confirmed at an industrial scale. It highlights the importance of accounting for seasonal moisture dynamics in operational planning, particularly for sawlog transport and sawn wood drying.

Based on these findings, this study offers direct recommendations for optimizing sawmill and forestry operations. Sawmills can refine their sorting and bucking strategies by implementing species-specific models that account for the different knot, sapwood, and MC characteristics. For instance, optimization software should treat sound and dead knots as separate variables to more accurately predict the structural grade of lumber from a given log. Operationally, acknowledging seasonal MC trends allows for better planning of log transport and more efficient energy management for sawn wood drying.

Future work will focus on developing predictive models/tools to estimate internal wood quality, enabling more advanced, multi-criteria optimization strategies in processing. The key next step is to link these models with forest growth simulators, establishing a fully digital value chain from forest to final product.

Author Contributions: T.R.: conceptualization, formal analysis, investigation, methodology, writing—original draft; J.-M.L.: conceptualization, funding acquisition, supervision, writing—review and editing; R.D.: conceptualization, funding acquisition, supervision, writing—review and editing; E.U.: resources, writing—review and editing; R.R.: supervision, writing—review and editing. All authors have read and agreed to the published version of the manuscript.

Funding: This research was funded by ANRT (Association Nationale de la Recherche et de la Technologie) via the CIFRE convention No. 2022/1404 and Groupe SIAT.

Data Availability Statement: The data that supports the findings of this study are available from the corresponding authors, T.R. and J.-M.L., upon reasonable request.

Acknowledgments: The authors thank Groupe SIAT for providing access to the production data. During the preparation of this manuscript, the authors used Gemini, version 2.5 Pro for the purposes of writing reformulations for English clarity and conciseness, assistance for debugging the R scripts for the graphics and statistical tests. The authors have reviewed and edited the output and take full responsibility for the content of this publication.

Conflicts of Interest: T.R. and R.D. are employed by Groupe SIAT company. E.U. is employed by MiCROTEC Bressanone, Italy, the company that designed and manufactured the industrial CT scanner used. Groupe SIAT and MiCROTEC provided the data. The other authors declare no competing interests.

Abbreviations

The following abbreviations are used in this manuscript:

CNN	Convolutional neural network
CT	Computed tomography
FSP	Fiber saturation point
ID	Infradensité (average basic density)
MC	Moisture content
SW	Sapwood width

Appendix A

The ANOVA type III on the interaction model = lm(sapwood_proportion ~ diameter * essence) showed that *p*-value for 'diameter:essence' is <0.05, so the assumption of parallel slopes is violated. Analyzing the interaction model was required, not a simpler ANCOVA model.

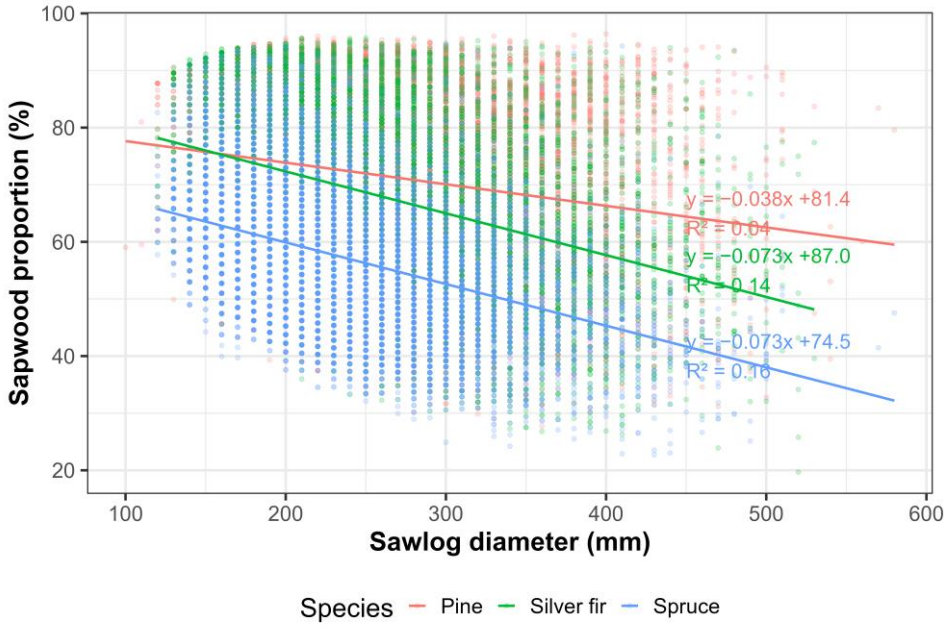

Figure A1. Scatterplot of sapwood proportion in function of the sawlog diameter by species. The slopes for spruce and silver fir are similar but differ from Pine.

Estimated slope analysis was obtained by the function: emtrends (interaction_model, ~ essence, var = "diameter") which output a diameter.trend of −0.0378, −0.0733 and −0.0729 respectively for pine, silver fir, and spruce. Table A1 shows the pairwise comparison by the function: pairs (slope_analysis, adjust = "tukey")

Table A1. Pairwise slope comparison for sapwood proportion vs. sawlog diameter by species.

Contrast	Estimate	*p*-Value
Pine—silver fir	0.035482	<0.0001
Pine—spruce	0.035141	<0.0001
Silver fir—spruce	−0.000341	0.9909

Appendix B

Table B1. Summary of models by knot types (sound and black) vs. sawlog diameter and mean knots diameter by species.

Knot Type	Models with Species Interaction	Analysis Parts	Term	Estimate	Std_Error	*p*-Value	Significance
Sound knots	SD vs. sawlog diameter	Coefficients	(Intercept)	−0.758	0.788	0.338	
			Diameter	0.034	0.002	<0.001	***
			Species: silver fir	0.628	1.13	0.579	
			Species: spruce	−0.007	1.142	0.995	
			Diameter × species: silver fir	−0.013	0.003	<0.001	***
			Diameter × species: spruce	−0.011	0.003	0.002	**

		Slope comparison	Pine—silver fir	0.0133	0.0034	<0.001	
			Pine—spruce	0.0111	0.0034	0.004	
			Silver fir—spruce	−0.0022	0.0034	0.798	
	SD vs. mean knot diameter	Coefficients	(Intercept)	−4.703	1.299	<0.001	***
			Mean sound knot diameter	0.406	0.035	<0.001	***
			Species: silver fir	0.051	2.113	0.981	
			Species: spruce	−5.234	2.853	0.069	.
			Mean diameter × species: silver fir	0.06	0.077	0.431	
			Mean diameter × species: spruce	0.371	0.124	0.003	**
		Slope comparison	Pine—silver fir	−0.0604	0.0765	0.71	
			Pine—spruce	−0.3708	0.1241	0.01	
			Silver fir—spruce	−0.3104	0.1371	0.065	
Black knots	SD vs. sawlog diameter	Coefficients	(Intercept)	7.469	0.624	<0.001	***
			Diameter	0.004	0.002	0.044	*
			Species: silver fir	−3.163	0.895	<0.001	***
			Species: spruce	−1.69	0.904	0.064	.
			Diameter × species: silver fir	−0.002	0.003	0.388	
			Diameter × species: spruce	−0.009	0.003	0.002	**
		Slope comparison	Pine—silver fir	0.0023	0.0027	0.663	
			Pine—spruce	0.0086	0.0027	0.005	
			Silver fir—spruce	0.0063	0.0027	0.056	
	SD vs. mean knot diameter	Coefficients	(Intercept)	7.232	0.828	<0.001	***
			Mean black knot diameter	0.061	0.034	0.077	.
			Species: silver fir	−2.378	1.271	0.064	.
			Species: spruce	−0.283	1.262	0.823	
			Mean diameter × species: silver fir	−0.065	0.066	0.327	
			Mean diameter × species: spruce	−0.245	0.072	<0.001	***
		Slope comparison	Pine—silver fir	0.0647	0.0658	0.589	
			Pine—spruce	0.2448	0.0723	0.003	
			Silver fir—spruce	0.1801	0.0849	0.09	

Signif. codes: 0 '***' 0.001 '**' 0.01 '*' 0.05 '.' 0.1 ' ' 1.

References

1. Mo, J.; Haviarova, E.; Kitek Kuzman, M. Wood-Products Value-Chain Mapping. *Wood Mater. Sci. Eng.* **2024**, *19*, 955–965. https://doi.org/10.1080/17480272.2024.2328787.
2. Jansson, G.; Hansen, J.K.; Haapanen, M.; Kvaalen, H.; Steffenrem, A. The Genetic and Economic Gains from Forest Tree Breeding Programmes in Scandinavia and Finland. *Scand. J. For. Res.* **2017**, *32*, 273–286. https://doi.org/10.1080/02827581.2016.1242770.
3. Fredriksson, M. Log Sawing Position Optimization Using Computed Tomography Scanning. *Wood Mater. Sci. Eng.* **2014**, *9*, 110–119. https://doi.org/10.1080/17480272.2014.904430.
4. Maness, T.C.; Adams, D.M. The Combined Optimization of Log Bucking and Sawing Strategies. *Wood Fiber Sci.* **1991**, *23*, 296–314; ISSN 0735-6161.
5. Rais, A.; Ursella, E.; Vicario, E.; Giudiceandrea, F. The Use of the first Industrial X-Ray CT Scanner Increases the Lumber Recovery Value: Case Study on Visually Strength-Graded Douglas-fir Timber. *Ann. For. Sci.* **2017**, *74*, 28. https://doi.org/10.1007/s13595-017-0630-5.
6. Müller, F.; Jaeger, D.; Hanewinkel, M. Digitization in Wood Supply—A Review on How Industry 4.0 Will Change the Forest Value Chain. *Comput. Electron. Agric.* **2019**, *162*, 206–218. https://doi.org/10.1016/j.compag.2019.04.002.

7. Smith, J.H.G.; Walters, J.; Wellwood, R.W. Variation in Sapwood Thickness of Douglas-fir in Relation to Tree and Section Characteristics. *For. Sci.* **1966**, *12*, 97–103. https://academic.oup.com/forestscience/article/12/1/97/4709492 (accessed on 9 September 2025).
8. Eckelman, C. *Wood Moisture Calculations*; Purdue University: West Lafayette, IN, USA, 1997; Volume FNR 156, pp. 1–18.
9. Gibbs, R.D. Studies of wood: ii. on the water content of certain canadian trees and on changes in the water-gas system during seasoning and flotation. *Can. J. Res.* **1935**, *12*, 727–760. https://doi.org/10.1139/cjr35-063.
10. Hein, S.; Mäkinen, H.; Yue, C.; Kohnle, U. Modelling Branch Characteristics of Norway spruce from Wide Spacings in Germany. *For. Ecol. Manag.* **2007**, *242*, 155–164. https://doi.org/10.1016/j.foreco.2007.01.014.
11. Ji, A.; Cool, J.; Duchesne, I. Using X-Ray CT Scanned Reconstructed Logs to Predict Knot Characteristics and Tree Value. *Forests* **2021**, *12*, 720. https://doi.org/10.3390/f12060720.
12. Gazo, R.; Wells, L.; Krs, V.; Benes, B. Validation of Automated Hardwood Lumber Grading System. *Comput. Electron. Agric.* **2018**, *155*, 496–500. https://doi.org/10.1016/j.compag.2018.06.041.
13. Roblot, G.; Coudegnat, D.; Bleron, L.; Collet, R. Evaluation of the Visual Stress Grading Standard on French spruce (*Picea excelsa*) and Douglas-fir (*Pseudotsuga menziesii*) Sawn Timber. *Ann. For. Sci.* **2008**, *65*, 812. https://doi.org/10.1051/forest:2008071.
14. Bhandarkar, S.; Luo, X.; Daniels, R.; Tollner, E. A Novel Feature-Based Tracking Approach to the Detection, Localization, and 3-D Reconstruction of Internal Defects in Hardwood Logs Using Computer Tomography. *Pattern Anal. Appl.* **2006**, *9*, 155–175. https://doi.org/10.1007/s10044-006-0035-9.
15. Pietikäinen, M. *Detection of Knots in Logs Using X-Ray Imaging*; VTT, Technical Research Centre of Finland: Espoo, Finland, 1996; ISBN 951-38-4924-4.
16. Gejdoš, M.; Gergeľ, T.; Michajlová, K.; Bucha, T.; Gracovský, R. The Accuracy of CT Scanning in the Assessment of the Internal and External Qualitative Features of Wood Logs. *Sensors* **2023**, *23*, 8505. https://doi.org/10.3390/s23208505.
17. Funck, J.W.; Zhong, Y.; Butler, D.A.; Brunner, C.C.; Forrer, J.B. Image Segmentation Algorithms Applied to Wood Defect Detection. *Comput. Electron. Agric.* **2003**, *41*, 157–179. https://doi.org/10.1016/S0168-1699(03)00049-8.
18. Breinig, L.; Berglund, A.; Grönlund, A.; Brüchert, F.; Sauter, U.H. Effect of Knot Detection Errors When Using a Computed Tomography Log Scanner for Sawing Control. *For. Prod. J.* **2013**, *63*, 263–274. https://doi.org/10.13073/FPJ-D-13-00068.
19. Gérardin, P.; Hentges, D.; Gérardin, P.; Vinchelin, P.; Dumarçay, S.; Audoin, C.; Gérardin-Charbonnier, C. Knotwood and Branchwood Polyphenolic Extractives of silver fir, spruce and Douglas fir and Their Antioxidant, Antifungal and Antibacterial Properties. *Molecules* **2023**, *28*, 6391. https://doi.org/10.3390/molecules28176391.
20. Willför, S.; Hemming, J.; Reunanen, M.; Eckerman, C.; Holmbom, B. Lignans and Lipophilic Extractives in Norway spruce Knots and Stemwood. *Holzforschung* **2003**, *57*, 27–36. https://doi.org/10.1515/HF.2003.005.
21. Holmbom, B.; Willfoer, S.; Hemming, J.; Pietarinen, S.; Nisula, L.; Eklund, P.; Sjoeholm, R. Knots in Trees: A Rich Source of Bioactive Polyphenols. In *Materials, Chemicals, and Energy from Forest Biomass*; ACS Symposium Series; American Chemical Society: Wahington, DC, USA, 2007; Volume 954, pp. 350–362, ISBN 978-0-8412-3981-4.
22. Kebbi-Benkeder, Z.; Colin, F.; Dumarçay, S.; Gérardin, P. Quantification and Characterization of Knotwood Extractives of 12 European Softwood and Hardwood Species. *Ann. For. Sci.* **2015**, *72*, 277–284. https://doi.org/10.1007/s13595-014-0428-7.
23. Johansson, E.; Johansson, D.; Skog, J.; Fredriksson, M. Automated Knot Detection for High Speed Computed Tomography on *Pinus sylvestris* L. and *Picea abies* (L.) Karst. Using Ellipse Fitting in Concentric Surfaces. *Comput. Electron. Agric.* **2013**, *96*, 238–245. https://doi.org/10.1016/j.compag.2013.06.003.
24. Xie, G.; Wang, L.; Williams, R.A.; Li, Y.; Zhang, P.; Gu, S. Segmentation of Wood CT Images for Internal Defects Detection Based on CNN: A Comparative Study. *Comput. Electron. Agric.* **2024**, *224*, 109244. https://doi.org/10.1016/j.compag.2024.109244.
25. Li, Z.; Jia, W.; Li, F.; Zhao, Y.; Guo, H.; Wang, F. A Study on the Variation of Knot Width in Larix Olgensis Based on a Mixed-Effects Model. *Comput. Electron. Agric.* **2025**, *234*, 110215. https://doi.org/10.1016/j.compag.2025.110215.
26. Fernández-Serrano, Á.; Villasante, A. Alterations to the Bending Mechanical Properties of *Pinus Sylvestris* Timber According to Flatwise and Edgewise Directions and Knot Position in the Cross-Section. *Maderas-Cienc. Tecnol.* **2024**, *26*, e4324. https://doi.org/10.22320/s0718221x/2024.43.
27. Loubère, M.; Saint-Andre, L.; Hervé, J.-C.; Vestøl, G. Relationships between Stem Size and Branch Basal Diameter Variability in Norway spruce (*Picea abies* (L.) Karsten) from Two Regions of France. *Ann. For. Sci.* **2004**, *61*, 525–535. https://doi.org/10.1051/forest:2004047.
28. Perre, P.; Keey, R. 40 Drying of Wood: Principles and Practices. In *Handbook of Industrial Drying*; CRC Press: Boca Raton, FL, USA, 2014. https://doi.org/10.1201/b17208-5344.

29. Zhang, Z.; Yang, X.; He, P.; Jiang, L. Simultaneous Density-Integral System for Estimating Stem Profile, Volume, Wood Density, and Biomass of Fourteen Tree Species in Northeast China. *Comput. Electron. Agric.* **2025**, *236*, 110453. https://doi.org/10.1016/j.compag.2025.110453.
30. Fredriksson, M. Predicting Strength of Norway spruce and Scots pine Sawn Timber Using Discrete X-Ray Log Scanning, Optical Board Scanning, Traceability, and Partial Least Squares Regression. *BioResources* **2024**, *19*, 1777–1788.
31. Ursella, E. In-Line Industrial Computed Tomography Applications and Developments. Ph.D. Thesis, Univertità Ca'Foscari Venezia, Venezia, Italy, 2021.
32. Trincado, G.; Burkhart, H.E. A Model of Knot Shape and Volume in Loblolly pine Trees. *Wood Fiber Sci.* **2008**, *40*, 634–646.
33. Billard, A.; Bauer, R.; Mothe, F.; Jonard, M.; Colin, F.; Longuetaud, F. Improving Aboveground Biomass Estimates by Taking into Account Density Variations between Tree Components. *Ann. For. Sci.* **2020**, *77*, 103. https://doi.org/10.1007/s13595-020-00999-1.
34. FCBA. Cubage des Bois Ronds et Assimiles. Available online: https://www.fcba.fr/ressources/fcba-info-cubage-des-bois-ronds-et-assimiles/ (accessed on 30 July 2025).
35. Glass, S.V.; Zelinka, S.L. Chapter 4: Moisture Relations and Physical Properties of Wood. In *Wood Handbook: Wood as an Engineering Material*; U.S. Department of Agriculture: Madison, WI, USA, 2021; p. 22.
36. Stamm, A.J. Shrinking and Swelling of Wood. *Ind. Eng. Chem.* **1935**, *27*, 401–406.
37. Cuny, H.; Leban, J.-M.; Hervé, J.-C.; Bontemps, J.-D.; Kerfriden, B.; Jacquin, P.; Lacarin, M.; Dauffy, V.; Duprez, C.; Wurpillot, S. XyloDensMap: A Georeferenced Dataset for the Wood Density of 110,000 Trees from 156 European Species in France. *Sci. Data* **2025**, *12*, 380. https://doi.org/10.1038/s41597-025-04645-1.
38. Posit team RStudio: Integrated Development Environment for R 2023. Posit Software, PBC, Boston, MA. Available online: https://www.posit.co/ (accessed on 9 September 2025).
39. Rust, S. Comparison of Three Methods for Determining the Conductive Xylem Area of Scots pine (*Pinus sylvestris*). *For. Int. J. For. Res.* **1999**, *72*, 103–108. https://doi.org/10.1093/forestry/72.2.103.
40. Longuetaud, F.; Mothe, F.; Leban, J.-M.; Mäkelä, A. *Picea abies* Sapwood Width: Variations within and between Trees. *Scand. J. For. Res.* **2006**, *21*, 41–53. https://doi.org/10.1080/02827580500518632.
41. Moberg, L. Models of Internal Knot Properties for *Picea abies*. *For. Ecol. Manag.* **2001**, *147*, 123–138. https://doi.org/10.1016/S0378-1127(00)00471-0.
42. Moberg, L. Models of Internal Knot Diameter for *Pinus sylvestris. Scand. J. For. Res.* **2000**, *15*, 177–187. https://doi.org/10.1080/028275800750014984.
43. Tomczak, K.; Tomczak, A.; Jelonek, T. Effect of Natural Drying Methods on Moisture Content and Mass Change of Scots pine Roundwood. *Forests* **2020**, *11*, 668. https://doi.org/10.3390/f11060668.
44. Elowson, T.; Bergström, M.; HämälÄinen, M. Moisture Dynamics in Norway spruce and Scots pine during Outdoor Exposure in Relation to Different Surface Treatments and Handling Conditions. *Holzforschung* **2003**, *57*, 219–227. https://doi.org/10.1515/HF.2003.032.
45. Trzcianowska, M.; LeBel, L.; Beaudoin, D. Performance Analysis of Log Yards Using Data Envelopment Analysis. *Int. J. For. Eng.* **2019**, *30*, 144–154. https://doi.org/10.1080/14942119.2019.1568035.
46. Jochen Schenk, H. Wood: Biology of a Living Tissue. *Am. J. Bot.* **2018**, *105*, 139–141. https://doi.org/10.1002/ajb2.1039.
47. Lee, N.-H.; Li, C.; Choi, J.-H.; Hwang, U.-D.; Jin, Y.-M. Determination of Trend of a Radial Distribution of Moisture Content within a Log Cross Section by Oven-Drying of Circumferential Slices (II)-for Some of Domestic Softwoods. *J. Korean Wood Sci. Technol.* **2004**, *32*, 19–25.
48. Département de la Santé des Forêts le Fome des Résineux 2019, Ministère de L'agriculture et de la Souveraineté Alimentaire. Available online: https://agriculture.gouv.fr/telecharger/150044 (accessed on 9 September 2025).
49. Hýsek, Š.; Löwe, R.; Turčáni, M. What Happens to Wood after a Tree Is Attacked by a Bark Beetle? *Forests* **2021**, *12*, 1163. https://doi.org/10.3390/f12091163.

Disclaimer/Publisher's Note: The statements, opinions and data contained in all publications are solely those of the individual author(s) and contributor(s) and not of MDPI and/or the editor(s). MDPI and/or the editor(s) disclaim responsibility for any injury to people or property resulting from any ideas, methods, instructions or products referred to in the content.